Neuron, Volume *95*

Supplemental Information

TDP-43 Depletion in Microglia Promotes Amyloid Clearance but Also Induces Synapse Loss

Rosa C. Paolicelli, Ali Jawaid, Christopher M. Henstridge, Andrea Valeri, Mario Merlini, John L. Robinson, Edward B. Lee, Jamie Rose, Stanley Appel, Virginia M.-Y. Lee, John Q. Trojanowski, Tara Spires-Jones, Paul E. Schulz, and Lawrence Rajendran

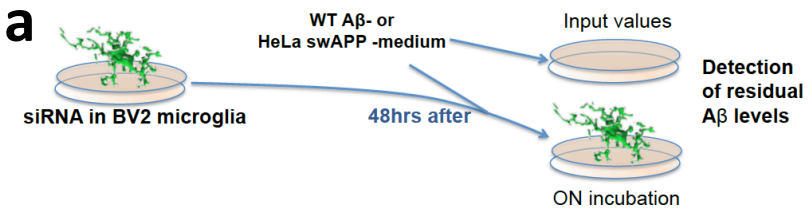

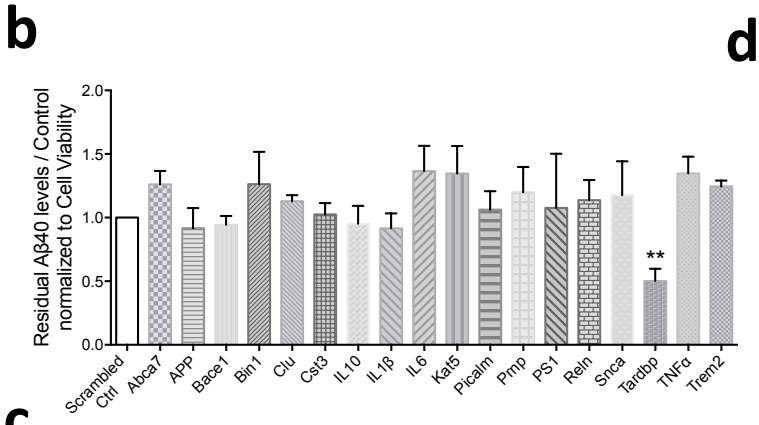

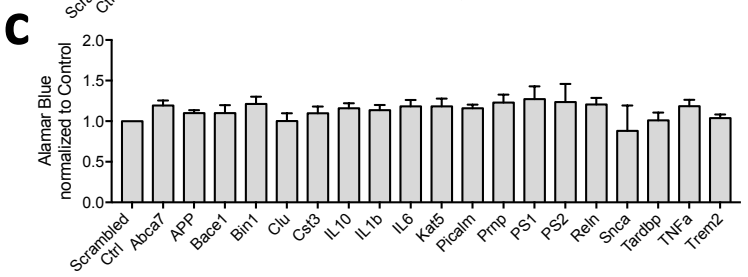

d

Number of families	1				
Number of comparisons per family	18				
Alpha	0.05				
Uncorrected Fisher's LSD	Mean Diff.	95.00% CI of diff.	Significant?	Summary	Individual P Value
Scrambled Ctrl vs. Abca7	-0.2612	-0.631 to 0.1085	No	ns	0.1632
Scrambled Ctrl vs. APP	0.0827	-0.3701 to 0.5355	No	ns	0.7168
Scrambled Ctrl vs. Bace1	0.05565	-0.4672 to 0.5785	No	ns	0.8325
Scrambled Ctrl vs. Bin1	-0.2632	-0.6766 to 0.1502	No	ns	0.2083
Scrambled Ctrl vs. Clu	-0.1291	-0.4988 to 0.2406	No	ns	0.4885
Scrambled Ctrl vs. Cst3	-0.02469	-0.3944 to 0.345	No	ns	0.8944
Scrambled Ctrl vs. IL10	0.04823	-0.3395 to 0.436	No	ns	0.8048
Scrambled Ctrl vs. IL1β	0.08454	-0.2852 to 0.4543	No	ns	0.6498
Scrambled Ctrl vs. IL6	-0.366	-0.7794 to 0.04736	No	ns	0.0818
Scrambled Ctrl vs. Kat5	-0.3468	-0.7346 to 0.04098	No	ns	0.0788
Scrambled Ctrl vs. Picalm	-0.06281	-0.4325 to 0.3069	No	ns	0.7358
Scrambled Ctrl vs. Prnp	-0.1992	-0.5689 to 0.1705	No	ns	0.2862
Scrambled Ctrl vs. PS1	-0.07573	-0.5986 to 0.4471	No	ns	0.7735
Scrambled Ctrl vs. Reln	-0.1371	-0.5504 to 0.2763	No	ns	0.5106
Scrambled Ctrl vs. Snca	-0.1762	-0.6991 to 0.3466	No	ns	0.5037
Scrambled Ctrl vs. Tardbp	0.4993	0.1295 to 0.869	Yes	**	0.0088
Scrambled Ctrl vs. TNFα	-0.348	-0.7177 to 0.02174	No	ns	0.0647
Scrambled Ctrl vs. Trem2	-0.2454	-0.6588 to 0.1679	No	ns	0.2404

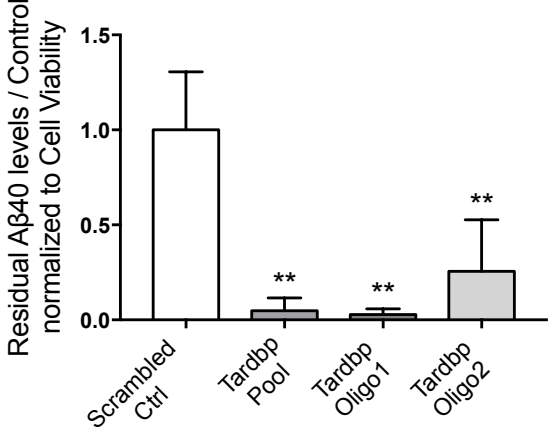

Supplementary Figure 1

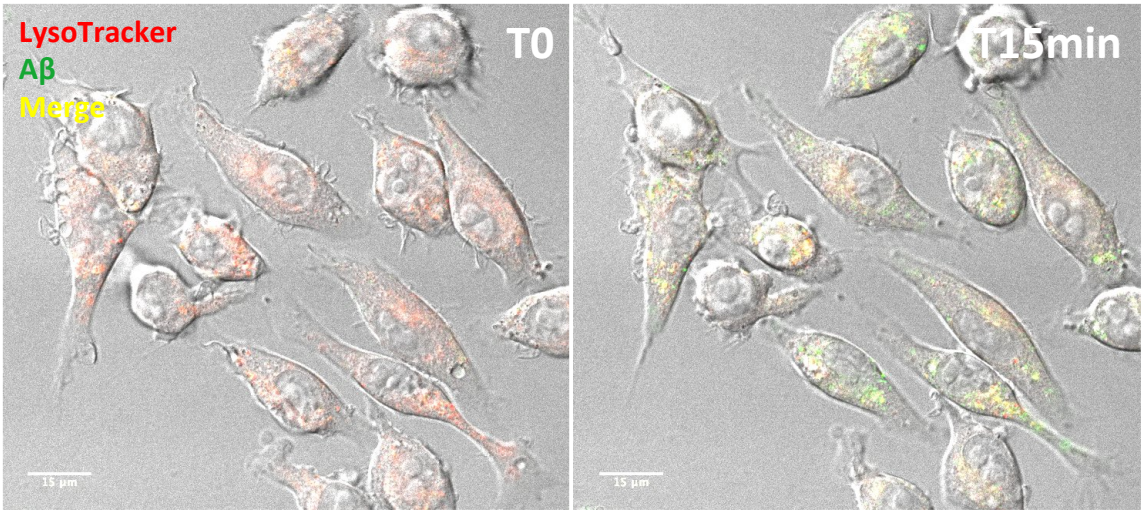

Supplementary Figure 2

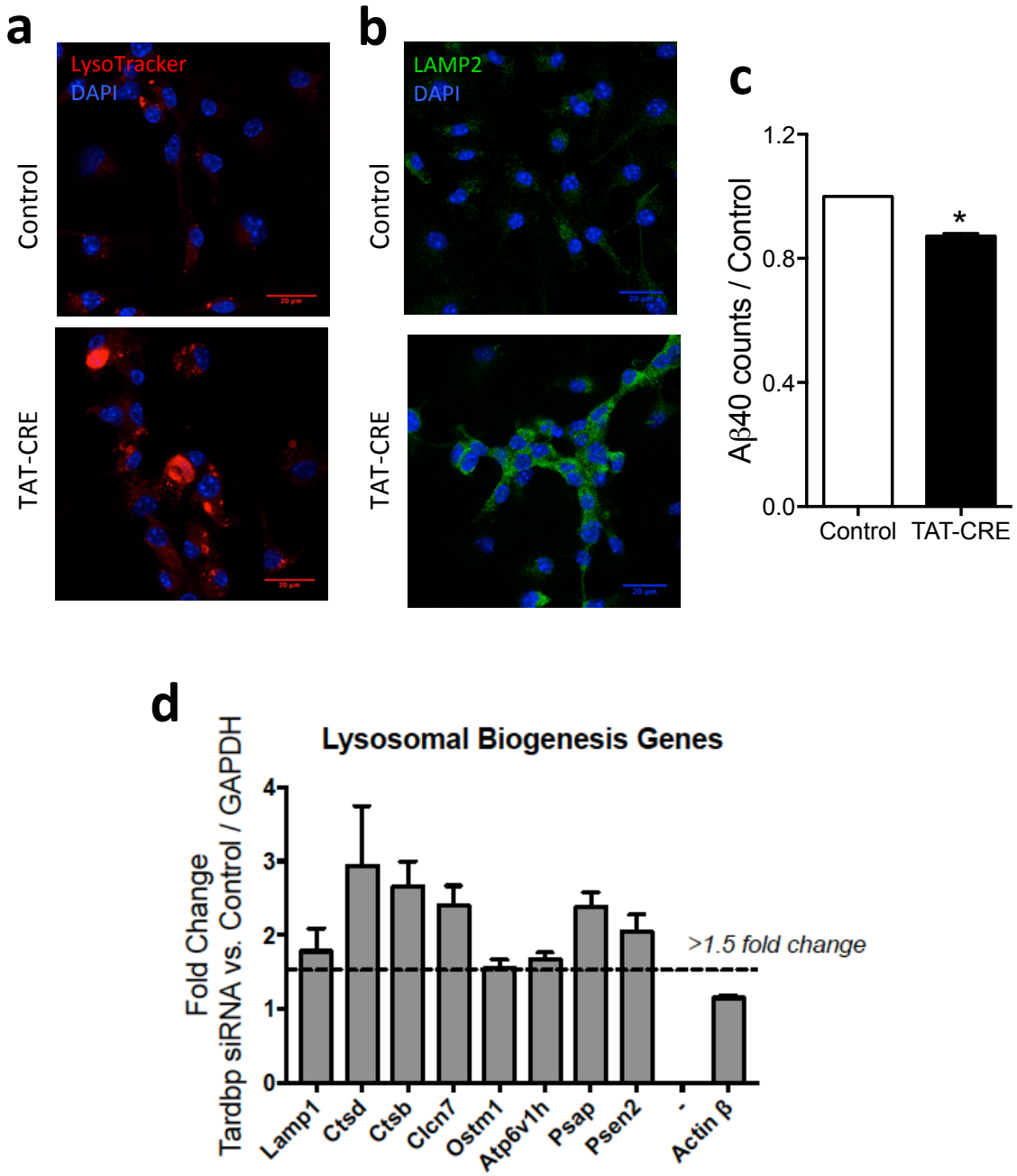

Supplementary Figure 3

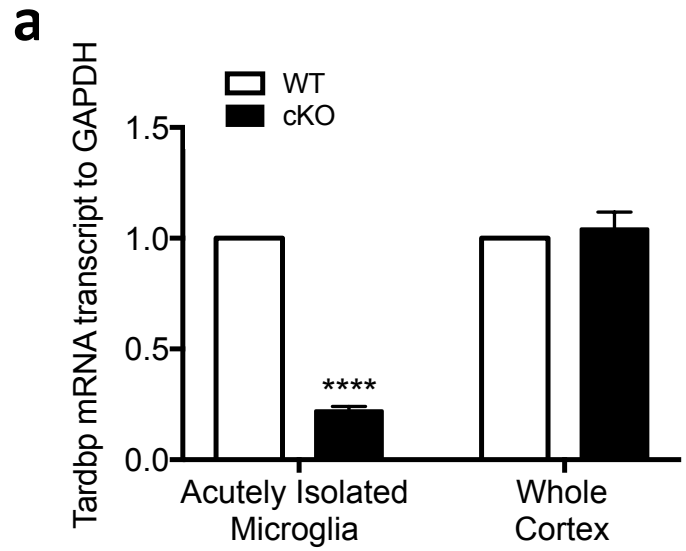

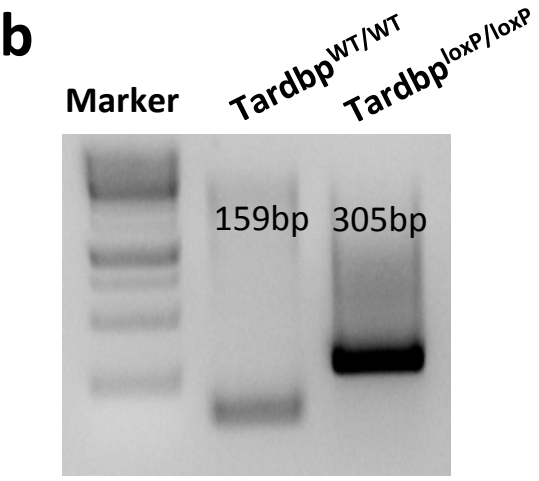

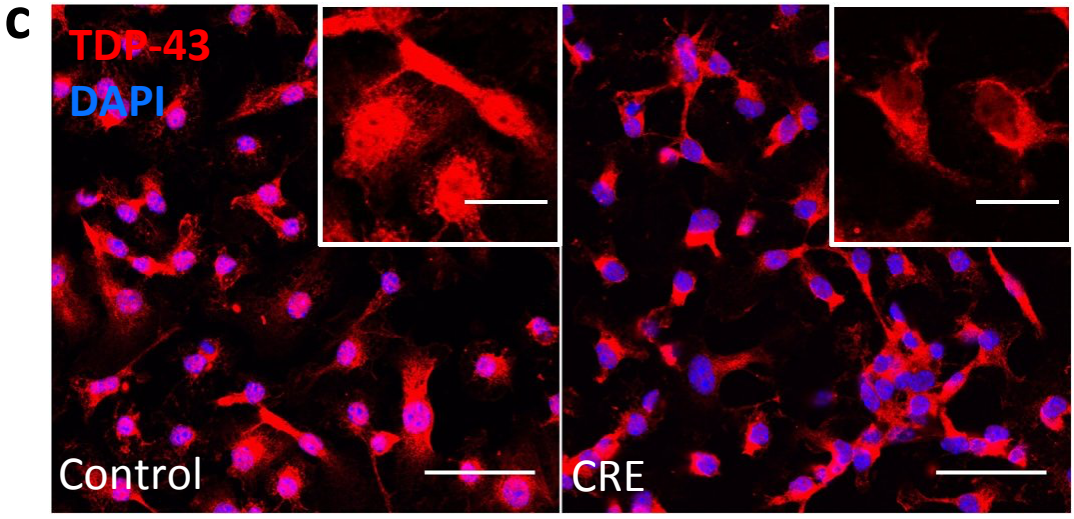

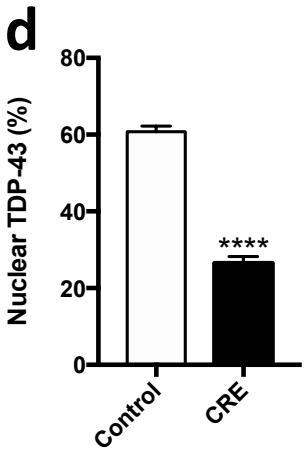

Supplementary Figure 4

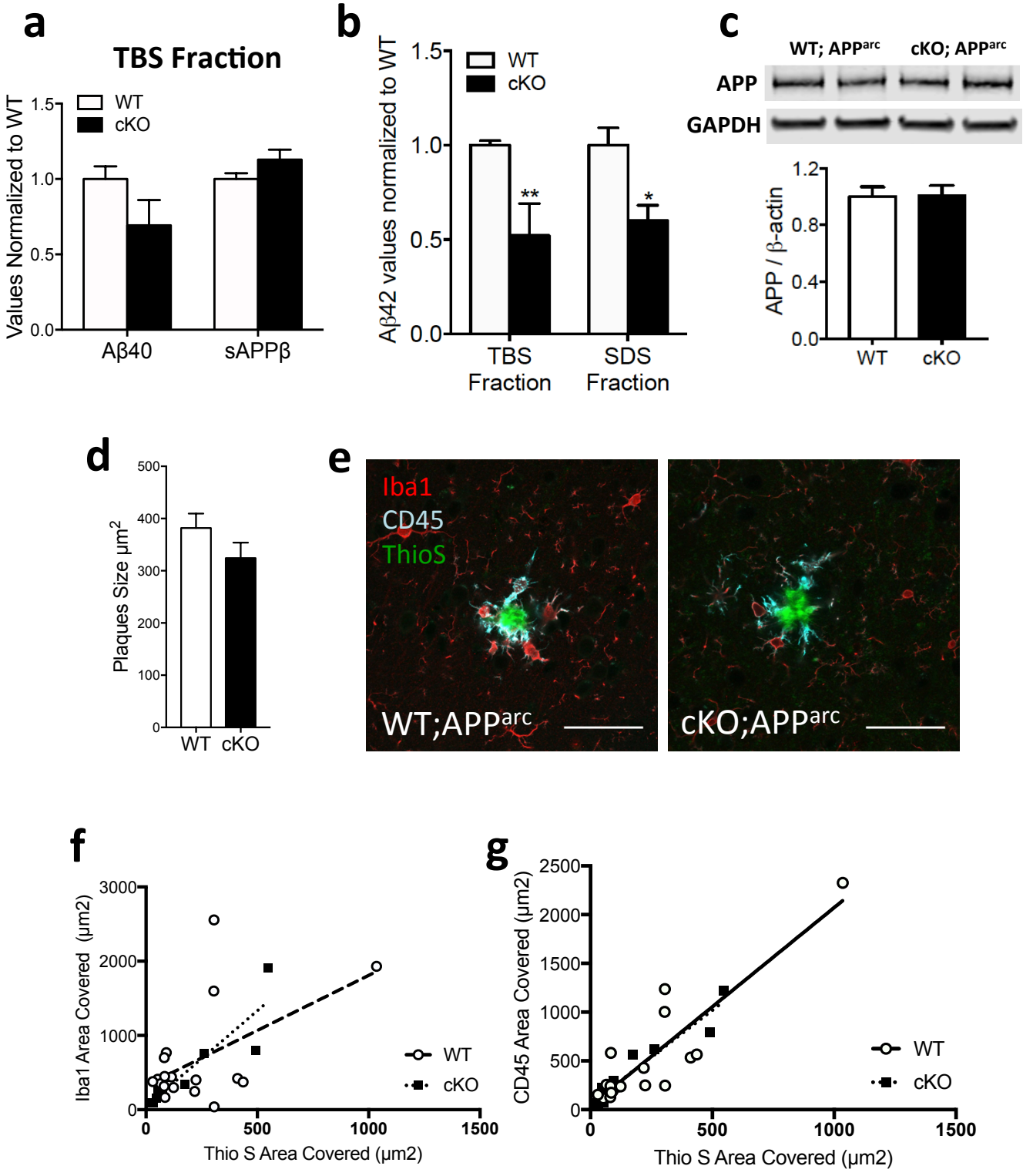

Supplementary Figure 5

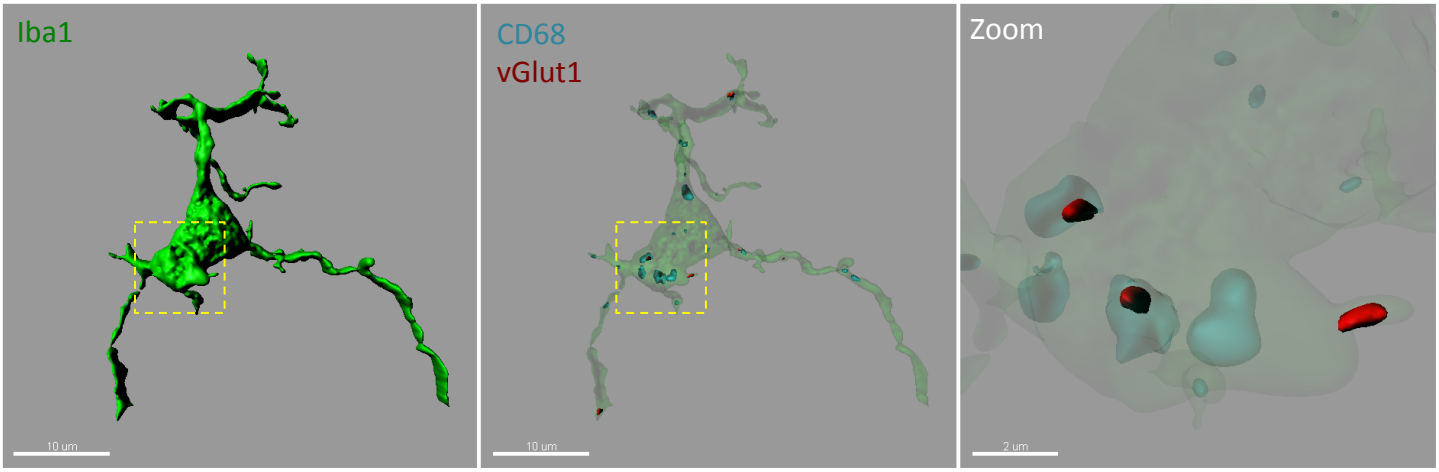

Supplementary Figure 6

Supplementary Figures Legends

Figure S1, related to Figure 1. Screen and identification of Tardbp

a, Aβ clearance assay in BV2 cells: the clearance capacity of microglia was measured by their capability to clear murine Aβ upon overnight incubation with WT primary neurons-conditioned medium. **b**, Knockdown screen for 18 genes associated with neurodegenerative disorders, assessed in Aβ clearance assay: residual murine WT Aβ levels were significantly reduced in Tardbp depleted cells compared to scrambled control (n=3-6, mean±sem ** $p<0.01$, one-way ANOVA, Uncorrected Fisher's LSD Test). **c**, cell viability assay ensuring no toxic effects due to genes knockdown. **d**, table reporting the p value for each comparison vs. control (n=3-6, mean±sem ** $p<0.01$, one-way ANOVA, Uncorrected Fisher's LSD Test).
e, Residual Aβ40 levels from HeLa swAPP conditioned medium, after overnight incubation with BV2 cells depleted of TDP-43, normalized to scrambled control and to cell viability (means±SEM, ** $p<0.005$, using one-way ANOVA followed by Dunnett's multiple comparison test).

Figure S2, related to Figure 1. Internalized Aβ colocalize with acidic vesicles

a, Representative confocal image of BV2 cells at T0 and after 15min incubation with pH sensitive dye LysoTracker (red) and fluorescently-labeled Aβ40 (green). Co-localization of the signals upon internalization is shown in yellow.

Figure S3, related to Figure 1. TDP-43 depletion promotes lysosomal biogenesis

a, Representative single focal plane micrographs for LysoTracker staining and **b**, immunohistochemistry against LAMP2 in $Tardbp^{floxed/floxed}$ primary microglia treated with control glycerol solution or recombinant CRE enzyme.

c, Quantification of Aβ clearance assay in control- or CRE-treated $Tardbp^{floxed/floxed}$ primary microglia, showing significant reduction in residual $A\beta_{40}$Swe levels normalized to control (mean±SEM, n=2; *p<0.05, using two-tailed unpaired t-test). **d**, Fold-change expression of TFEB-regulated genes in BV2 cells depleted of TDP-43, as compared to scrambled control, normalized to GAPDH reference gene (>1.5 fold change cutoff, mean±SEM, n=2)

Figure S4, related to Figure 2. Validation of microglial TDP-43 depletion in Tardbp floxed mice

a, RT-PCR detection of Tardbp mRNA transcripts normalized to Gapdh reference gene in an acutely isolated microglia population (pool of 4 brains per experiment, n=2 or in whole cortex from WT (n=3) or cKO (n=3) mice. ****p<0.0001 by two-way ANOVA, followed by uncorrected Fisher's LSD test. **b**, PCR from genomic DNA extracted by acutely isolated microglia confirming the presence of floxed Tardbp sequence in cKO samples compared to WT. **c**, Representative single focal plane micrographs for TDP-43 immunopositive signal, in control- or CRE-treated $Tardbp^{floxed/floxed}$ primary microglia. Scale bar, 40µm. Inset, scale bar, 15µm. **d**, Quantification of nuclear TDP-43 signal, shown as percentage of the nuclear area, in control- (n=200) or CRE-treated (n=173) $Tardbp^{floxed/floxed}$ primary microglia (mean±SEM, n=3 per treatment, ****p<0.0001, using two-tailed unpaired t-test).

Figure S5, related to Figure 3. Reduced amyloid levels in cKO mice

Multiplexed electrochemoluminescent ELISA measurement of **a**, Aβ40 and sAPPβ levels in the TBS-fraction from App^{arc};WT and cKO cortex homogenates (mean±SEM, n=4 mice per genotype) and **b**, Aβ42 levels in the TBS- and SDS-fraction of the same samples (mean±SEM, **p<0.01, *p<0.05, by two-way ANOVA, followed by uncorrected Fisher's LSD test). **c**, Representative western blots for APP detection in cortex of App^{arc};WT and cKO mice, and relative quantification (mean±SEM, n=4 mice per genotype). **d**, Quantification of plaque size in the cortex of App^{arc};WT and KO mice (WT n=158, cKO n=73 plaques) **e**, Representative max-projections of confocal stacks, acquired from cortex of WT;APP^{arc} or cKO;APP^{arc} adult mice, stained for amyloid plaques (ThioS) and immunostained for microglia markers (Iba1, CD45). Scale bar, 50µm. **f,** Positive correlation between plaque size/ThioS and Iba1 or **g**, plaque size/ThioS and CD45 staining is not different between genotypes, as shown by linear regression analysis. Mean±SEM, WT n=18, cKO n=10 plaques; 4 animals per genotype.

Figure S6, related to Figure 4. Engulfment of synaptic markers by microglia

Representative 3D reconstruction of a single microglia cell acquired by confocal microscopy from the somatosensory cortex of a $Cx3cr1^{CreER}$;$Tardbp^{+/+}$ mouse. The reconstruction shows vGlut1 immunoreactive puncta localized within CD68-positive phagocytic structure, inside an Iba1-positive microglia.

Supplementary Table 1, related to Figure 5a,b
Detailed information related to the ALS cohort selected for the clinical study.

	ALS (65-74 yrs)			ALS (≥75 yrs)		
	with AD (n=25)	without AD (n=505)	p value	with AD (n=12)	without AD (n=156)	p value
Gender % male	48	59.8	0.167	83.3	48.7	0.02*
Race % Caucasian	88	91.7	0.496	91.7	94.9	0.677
ApoE genotype % ApoE4 (3/4, 4/4)	45.5	28	0.132	16.7	22.4	0.232
Type of symptom onset % Bulbar	56	33.7	0.067#	50	41.9	0.4
Survival in years mean±SD	1.97±0.801	2.91±1.635	0.134	3.04±2.52	2.59±1.94	0.57
MMSE mean±SD	26.5±0.58	27.38±2.86	0.542	22.5±0.71	26.15±2.29	0.135
Years of education mean±SD	15.8±1.56	14.16±0.19	0.22	14±2.00	13.26±0.48	0.70

Supplementary Table 2, related to Figure 5e-g
Detailed information related to the human post-mortem samples used for CD68, and pTDP-43-Iba1 colocalization study.

Edinburgh Brain Bank Identifier	MRC Unique Identifier	Diagnosis	Age	Sex
SD001-16	BBN001.28406	Healthy Control	79	M
SD017-16	BBN001.28793	Healthy Control	79	F
SD018-16	BBN001.28794	Healthy Control	79	F
SD024-15	BBN001.26495	Healthy Control	78	M
SD051-15	BBN001.28402	Healthy Control	79	M
SD063-13	BBN_19686	Healthy Control	77	F
SD002-16	BBN001.28407	ALS	67	F
SD004-16	BBN001.28409	ALS	62	F
SD010-14	BBN_20604	ALS	62	F
SD014-14	BBN_20613	ALS	50	M
SD016-14	BBN_20993	ALS	43	M
SD018-15	BBN_25742	ALS	58	M
SD021-15	BBN_26494	ALS	60	M
SD026-15	BBN001.26125	ALS	49	F
SD027-14	BBN_22225	ALS	62	M
SD027-15	BBN001.26126	ALS	71	M
SD029-15	BBN001.26098	ALS	59	F
SD030-15	BBN001.26128	ALS	74	M
SD033-15	BBN001.26497	ALS	63	F
SD036-15	BBN001.26498	ALS	78	M
SD041-14	BBN_24218	ALS	68	M
SD045-15	BBN001.26729	ALS	83	F
SD046-15	BBN001.26730	ALS	54	M
SD047-13	BBN_18803	ALS	75	F
SD048-14	BBN_24321	ALS	63	F
SD049-13	BBN_18806	ALS	60	M
SD049-15	BBN001.26765	ALS	66	F
SD052-13	BBN_18807	ALS	65	F
SD053-13	BBN_19689	ALS	89	M
SD057-13	BBN_19688	ALS	57	M
SD058-13	BBN_20616	ALS	40	F
SD059-13	BBN_20617	ALS	71	M
SD059-14	BBN_24669	ALS	64	M